Design of a Magnetic Bearing

Design of a Magnetic Bearing

S.A.J. Hol[1], J.C. Compter[2], A.J.A. Vandenput[3], R. Munnig-Schmidt[4]

[1] ASML (Veldhoven), TU/e (Eindhoven); [2] Philips (Eindhoven), TU/e;

[3] TU/e; [4] ASML

Abstract

A popular approach to nano-positioning requirements in precision engineering in general and micro-lithography in particular is to subdivide the stage positioning architecture into a coarse positioning module with micrometer accuracy (Long Stroke), onto which a fine positioning module (Short Stroke) is cascaded. The latter is responsible for correcting the residual error of the coarse positioning module to the last nanometers. High accuracy positioning in 6 Degrees Of Freedom put severe constraints on the actuators and/or bearing systems. Actuators are used for generating a varying force being part of a control loop. Bearing systems should generate a force as constant as possible in the bearing direction, but the force perpendicular to that direction should be as low as possible. Actuators could serve as a bearing system, but on the one hand this would require the actuators to be large and thus heavy and on the other hand a substantial amount of heat is continuously dissipated in order to generate the static forces. Such heat generation does not contribute to the positioning performance of the actuators, but significantly affects the thermal stability of the application. The latter implication will be overcome if the bearing system is established by a system with permanent magnets.

Magnetics

Magnetic fields in free space

Magnetic (and electric) fields satisfy the Maxwell relations [1]:

$$\nabla \times \bar{H} = \bar{J} + \frac{\partial \bar{D}}{\partial t} \tag{1}$$

$$\nabla \times \bar{E} = -\frac{\partial \bar{B}}{\partial t} \tag{2}$$

$$\nabla \cdot \bar{B} = 0 \tag{3}$$

$$\nabla \cdot \bar{D} = \rho_v \tag{4}$$

with $\bar{H}$ the magnetic field strength, $\bar{B}$ the magnetic induction, $\bar{E}$ the electric field strength, $\bar{D}$ the electric field density, $\bar{J}$ the current density and ρ_v the spatial charge distribution. Helmholtz's theorem states that a vector potential can be defined for vector fields $\bar{\Psi}$ when $\nabla \cdot \bar{\Psi} = 0$. Since this is the case for the magnetic induction $\bar{B}$ (3), the magnetic vector potential $\bar{A}$ is defined as [2]:

$$\bar{B} = \nabla \times \bar{A} . \tag{5}$$

The magnetic vector potential $\bar{A}$ in a point at distance r due to the current density $\bar{J}$ through a volume V_c yields [3]:

$$\bar{A} = \frac{\mu_0}{4\pi} \iiint_{V_c} \frac{\bar{J}(\bar{r}')}{\left|\bar{r} - \bar{r}'\right|} dV(\bar{r}') \tag{6}$$

Applying (5) on (6) results in the Biot-Savart law, expressing the magnetic induction as a function of a current distribution through space:

$$\bar{B} = \frac{\mu_0}{4\pi} \iiint_{V_c} \frac{\bar{J}(\bar{r}') \times (\bar{r} - \bar{r}')}{\left|\bar{r} - \bar{r}'\right|^3} dV(\bar{r}') \tag{7}$$

Forces due to fields

Once the magnetic induction through space is know (7), the forces due to these fields can be determined by three methods [5, 6]: Lorentz's law, Maxwell stresses and the energy method. During this analysis Lorentz's law is used:

$$\bar{f} = \rho_v \cdot \left(\bar{E} + \bar{v} \times \bar{B} \right) = \rho_v \cdot \bar{E} + \bar{J} \times \bar{B} \tag{8}$$

in which $\bar{f}$ represents the force density.

Stability of magnetic systems; Earnshaw's theorem

Earnshaw erroneously stated that magnetic systems comprising permanent magnets are always non-stable. Successors refined his theorem: in [7] is proven that $\nabla \cdot \bar{f} < 0$ when materials with $\mu_r > 1$ are used and that $\nabla \cdot \bar{f} = 0$ when only materials with $\mu_r = 1$ are present around the magnetic sources:

$$\forall \mu_r = 1 \Rightarrow \nabla \cdot \bar{f} = \frac{\partial \bar{f}}{\partial x} + \frac{\partial \bar{f}}{\partial y} + \frac{\partial \bar{f}}{\partial z} = 0 \tag{9}$$

From (9) is concluded that if in one direction a positive stiffness ($\partial \bar{f} / \partial x$) is experienced at least in one direction a negative stiffness will occur.

Bearing System Specifications

The main function of the bearing system is to generate a force in one degree of freedom, consisting of a static force and a controllable dynamic force. The following table expounds the main specifications for the design:

Property	Value	Unit	Property	Value	Unit
Static force ($F_{z,static}$)	85	[N]	Motion range1 (x,y,z)	3,3,2	[mm]
Dynamic force ($F_{z,dynamic}$)	±20	[N]	Maximal stiffness2	500	[N/m]
Maximal mover mass	0.5	[kg]	Maximal damping[2]	0.2	[Ns/m]
Maximal stator mass	1.0	[kg]	Maximal dissipation3	40	[W]

Bearing System Modelling

In the design process an analytical model, a numerical model (boundary element model) and a prototype were used. As shown in Fig. 1 the configuration consists of two vertically magnetised rings, a coil connected to the stator and two radially magnetised rings connected to the mover.

1 Required stroke of mover with respect to the stator
2 Cross talk between mover and stator
3 When the dynamic force is 20 [N]

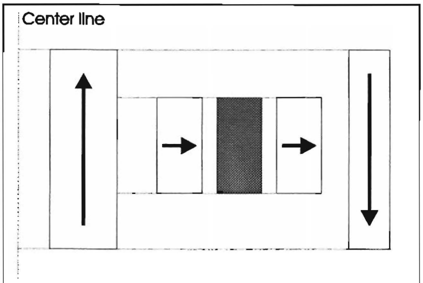

Figure 1: Configuration of the system

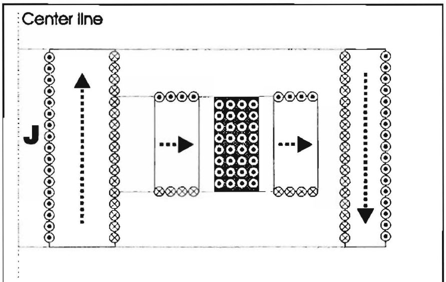

Figure 2: Current sheets as magnet

Analytical Model

In order to determine the force on the mover magnets due to the stator magnets the latter are modelled as current sheets as shown in Fig. 2. Applying (7) on these current distributions the radial component of the induction due to the stator magnets is determined [4]:

$$B_r = a \cdot \sqrt{\frac{R_1}{r}} \cdot \frac{2}{k}\left[\left(1-\frac{k^2}{2}\right)K(k) - E(k)\right]_{k_+}^{k_-} \tag{10}$$

in which $a = \mu_0 \frac{\sum i}{4\pi h_1}$, $k_\pm = \sqrt{\frac{2}{1+\beta+\delta_\pm^2}}$, $\beta = \frac{R_1^2 + r^2}{2R_1 r}$, $\delta_\pm = \frac{u_\pm}{\sqrt{2R_1 r}}$, $u_\pm = z \pm h$ and for the elliptic integrals K and E one yields:

$$K(k) = \int_0^{\frac{\pi}{2}} \frac{d\varphi}{\sqrt{1-k^2 \sin^2 \varphi}} \tag{11}$$

$$E(k) = \int_0^{\frac{\pi}{2}} \sqrt{1-k^2 \sin^2 \varphi} \cdot d\varphi \tag{12}$$

Once B_r is known the vertical force on the moving magnets is calculated by (8) when these magnets are modelled as current distributions as well. The same is done for the force on the moving magnets due to the current conducting coil. The dissipation due to the current density ($J(r')$) in the coil (V_c) with resistance (ρ) is determined by:

$$P(J) = \iiint_{V_c} \rho \cdot J(r')^2 \cdot dV(r') \tag{13}$$

Numerical Model

The same model was numerically analysed by the boundary element method. The relative permeability (μ_r) of the magnets was chosen to be μ_r=1, according to the analytical model. In practice this value will be 1.02<μ_r<1.35. The moving magnets were displaced 1 [mm] from their zero position in vertical direction. The force was evaluated during this displacement for both the analytical and numerical model. The static and dynamic forces are shown in Fig. 3 (differences between the models are <0.01% and are attributed to the numeric accuracy).

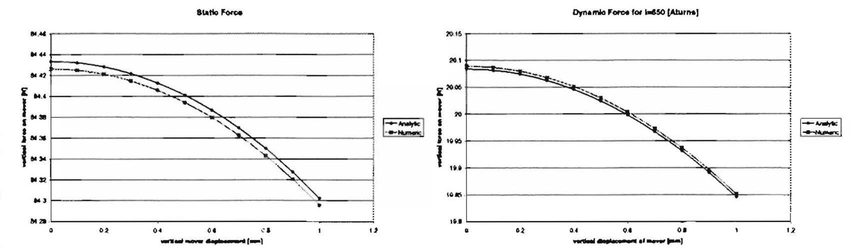

Figure 3: Static and dynamic force on the mover for different vertical displacements

Prototype

In Fig. 4 the prototype of the design is shown. The permanent magnet segments are visible in the stator housing. The remanent induction of the magnets was the same as in the models, but μ_r=1.05. The following table lists the performance of all the models.

Property	Analytical Value	Numerical Value	Prototype Value	Unit
Static force ($F_{z,static}$)	84.4	84.4	82.2	[N]
Dynamic force ($F_{z,dynamic}$)	±20	±20	±20	[N]
Maximal stiffness in range	250	160	55	[N/m]
Dissipation for $F_{z,dynamic}$=20 [N]	33.8	33.8	33.3	[W]

From the table is concluded that the force generated by the prototype is slightly smaller than that of the model. Explanation is found in the fact that the coersitive field strength of the prototype magnets is smaller (since μ_r=1.05) resulting in a lower field density ($\overline{B}$) and therefore a lower force ($\overline{f}$) and magnet dimensions.

Comments and Conclusion

Analytical and numerical models were developed to design a bearing system. These models were used for a mutual comparison and a proto type was built to verify both models. The models turned out to be consistent with each other and the prototype. The realised design is a sub-optimal design. Future analysis will focus on the algorithm for finding an ultimate optimal design.

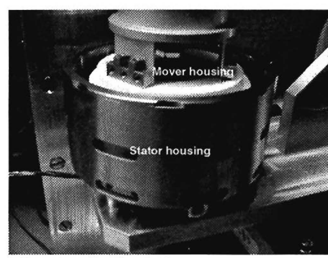

Figure 4: Prototype

References

[1] Binns, et al: The analytical and numerical solution of electric and magnetic fields, Wiley and Sons, 1995
[2] Cheng: Fundamentals of Engineering Electromagnetics, Addison, 1993
[3] Demarest: Engineering Electromagnetics, Prentice-Hall International, 1998
[4] Haas: Kräfte zwischen koaxialen Zylinderspulen, Elektrotechnik Archiv, 1976
[5] Hol: Design of a planar drive system, TU/e, 1999
[6] Kamerbeek: On the theoretical and experimental determination of the electromagnetic torque in electrical machines, TH Eindhoven, 1970
[7] Nijsse: Linear motion systems, TU-Delft, 2001